Renormalized tunneling of off-center impurities in alkali halides

Herbert B. Shore*
Department of Physics, University of California, San Diego, La Jolla, California 92037

Leonard M. Sander
Department of Physics, University of Michigan, Ann Arbor, Michigan 48104

(Received 18 September 1974)

The renormalization of tunneling matrix elements of off-center impurities in alkali halides due to interaction with lattice displacements is studied. The possible forms of interaction between nearest-neighbor lattice ions and impurities oriented along [100], [110], or [111] directions are enumerated. The renormalization factors are expressed in terms of sums over normal modes of the perfect lattice and reduced coupling coefficients describing the impurity-lattice interaction. The lattice sums are tabulated for nine alkali halides and the coupling coefficients are expressed in terms of measurable quantities: the impurity electric dipole moment and stress splitting factors. The results are applied to several experiments: the 90° reorientation of [100]-directed OH^- dipoles in several alkali halides, the 60° and 90° reorientation of [110]-directed Ag^+ in RbCl and RbBr (see previous paper), and the reorientation of O_2^- and N_2^- in KCl and KI. It is found that in general the relaxation rate can be qualitatively related to the reduction in matrix element due to renormalization.

I. INTRODUCTION

It has long been recognized that lattice interactions play a central role in determining the dynamics of paraelectric impurities in alkali halides.[1-3] Qualitatively, the nature of the interaction is as follows: A paraelectric impurity has the ability to reorient, i.e., change the direction of its electric-dipole moment. If the impurity distorts the lattice significantly in its initial position, when it reorients, the distortion must change. It is possible that in many cases the lattice distortions are reasonably large; thus any sensible description must treat them carefully, and, in particular, find how they follow the rotating impurity.

The most dramatic evidence to date for strong lattice coupling in a paraelectric system are the relaxation-time data of Kapphan for OH^- in RbBr.[4] Two analyses of these data have appeared: Dick and Strauch[5] attempted a microscopic description of the relaxation using the shell model for the phonons and perturbation theory for the lattice interaction. The present authors gave the second treatment in which shell-model phonons were incorporated into a theory valid for any strength coupling.[6] The theory was based on earlier work by the present authors[7,8] and by Pirc and Gosar.[9,10] This approach emphasized two separate effects of the phonons: first, the so called renormalization of the tunneling parameter,[11,12] that is, the replacement of the rigid-lattice reorientation rate Δ_0 by an effective tunneling rate Δ given by

$$\Delta^2 = \Delta_0^2 e^{-W_0} .$$

The parameter W_0 is a kind of Debye-Waller factor which depends on the lattice coupling. Second, the lattice affects the reorientation rate by providing a mechanism for releasing energy: The reorientation can be accompanied by the emission and absorption of phonons.

The calculation of Ref. 6 is satisfactory in that it can fit the data by using a few parameters which are not inconsistent with other experimental information. However, the mass of information computed to fit the complete relaxation-time–versus–temperature plot tends to obscure the fundamental physics. It would be very desirable to characterize the lattice effects on reorientation in some way which would allow us to quickly assess trends and compare different materials. The single parameter W_0 is the sort of information we need. If different materials have roughly the same bare tunneling parameter, then *low-temperature rates* will be determined mainly by W_0. It is the purpose of this paper to make it possible to calculate the W_0's for all the alkali halides and for paraelectric impurities whose equilibrium orientation is along [100], [110], or [111] crystal axes (this covers all the known cases).

We give in Sec. II a discussion of the model Hamiltonian we adopt. In this section we derive the W_0's from two types of information: information about the host lattice, and parameters characterizing the coupling. In Sec. III the calculation of host-lattice parameters using the shell model is discussed and the results listed. In Sec. IV we derive reduced coupling coefficients which are used to express W_0 in terms of a few parameters, one for each mechanism of lattice coupling.

In most previous work two main sorts of coupling mechanism have been considered: coupling of the impurity electric-dipole moment to lattice polar-

ization, and coupling of the so-called elastic-dipole tensor[13,14] to lattice strains. These are the mechanisms we consider here, and in Sec. V we express the relevant reduced coupling constants in terms of the electric-dipole moment of the impurity and the two stress-splitting coefficients, all of which are measured in standard experiments.

The central result of this paper is Eq. (26) of Sec. V which gives W_0 as the sum of three terms, W_{E_g}, $W_{T_{1u}}$, $W_{T_{2g}}$. In order to use the equation, only the elastic constants of the crystal, the dipole moment of the impurity, and the stress-splitting coefficients need be known. Then Eq. (26) together with Tables I, II, and IV give W_0 for a reorientation between any of the equivalent positions of an impurity.

Applications of the results are given in Sec. VI; first to interpret experiments on the relaxation of OH^- in various hosts,[4] second to explain some remarkable data on the relaxation of Ag^+ in RbCl and RbBr,[15,16] and finally to briefly examine the relaxation of other [110]-directed impurities.

In Sec. VII we discuss our approximations, and summarize the calculations.

II. THEORY

The major assumption made in the following calculation is that the impurity interacts only with its nearest neighbors. For the case of elastic-dipole interaction, this assumption is justified on the basis of the short range of the force. For the electric-dipole interaction, there is no *a priori* justification. However, the calculation of Ref. 6, in which an electric-dipole interaction falling off as R^{-3} was used, gives results for the renormalization factors that are within 10% of the values calculated in this paper.

A further assumption is that the phonon frequency spectrum is not perturbed by the presence of the impurity; i.e., that the interaction between the impurity and the lattice is linear.

We first derive a general expression for the renormalization factor in terms of the impurity-lattice coupling coefficients. The numbering of the six nearest neighbors and the coordinate system are shown in Fig. 1. The coordinates of the displacements of the nearest neighbors from their equilibrium positions form an 18-dimensional coordinate space with basis vectors $u_1^x, u_1^y, \ldots, u_6^y, u_6^z$. Linear combinations of these coordinates can be formed that transform as irreducible representations of the octahedral group O_h. Besides the three combinations that transform as a pure translation (T_{1u}) and the three that transform as a pure rotation (T_{1g}), the 12 remaining fall into the representations A_{1g}, E_g, T_{1u}, T_{2g}, and T_{2u}. The local distortions of the lattice produced by the first four of these representations correspond to, respectively, the breathing mode, uniaxial strain, electric dipole, and shear strain. The T_{2u} mode does not have a simple macroscopic interpretation. Pictorial representations of these modes are given in Fig. 2. The symmetry coordinates can be written out explicitly:

$$u^1_{A_{1g}} = 6^{-1/2}(u_1^z - u_2^z + u_3^x - u_4^x + u_5^y - u_6^y)\,, \tag{1a}$$

$$u^1_{E_g} = \tfrac{1}{2}(u_3^x - u_4^x - u_5^y + u_6^y)\,, \tag{1b}$$

$$u^2_{E_g} = 12^{-1/2}(2u_1^z - 2u_2^z - u_3^x + u_4^x - u_5^y + u_6^y)\,, \tag{1c}$$

$$u^1_{T_{1u}} = 12^{-1/2}(2u_3^x + 2u_4^x - u_1^x - u_2^x - u_5^x - u_6^x)\,, \tag{1d}$$

$$u^1_{T_{2g}} = \tfrac{1}{2}(u_3^y - u_4^y + u_5^x - u_6^x)\,, \tag{1e}$$

$$u^1_{T_{2u}} = \tfrac{1}{2}(u_3^z + u_4^z - u_5^z - u_6^z)\,. \tag{1f}$$

The remaining coordinates $u^2_{T_{1u}}$, $u^3_{T_{1u}}$, $u^2_{T_{2g}}$, $u^3_{T_{2g}}$, $u^2_{T_{2u}}$, $u^3_{T_{2u}}$ can be obtained from those listed by symmetry.

The dipole-lattice Hamiltonian can be written

$$\mathcal{H} = \mathcal{H}_e + \mathcal{H}_T + \mathcal{H}_p + \mathcal{H}_I\,. \tag{2}$$

Here $\mathcal{H}_e$ is a diagonal matrix representing the interaction of the dipole with an external electric field; $\mathcal{H}_T$ is an off-diagonal matrix containing the "bare" tunneling matrix elements; $\mathcal{H}_p = \sum_k \hbar\omega_k a_k^\dagger a_k$ is the unperturbed-phonon Hamiltonian; and $\mathcal{H}_I$ is the dipole-lattice interaction term. The dimensionality of the matrix and the number of independent tunneling parameters depends on whether one is considering [100]-, [110]- or [111]- directed impurities; at this point we keep the discussion general. The interaction term $\mathcal{H}_I$ is also a diagonal matrix:

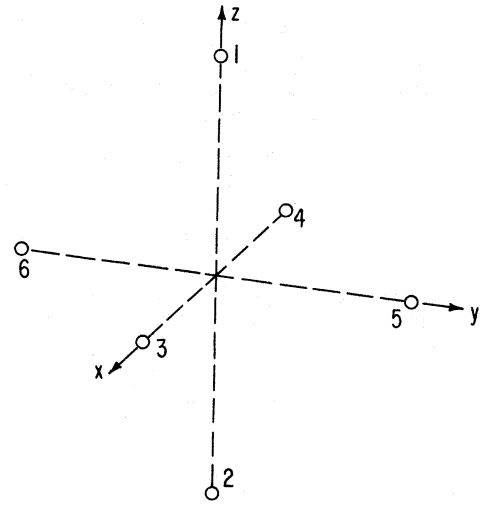

FIG. 1. Description of the coordinate axes and numbering system to describe the six nearest neighbors of the defect.

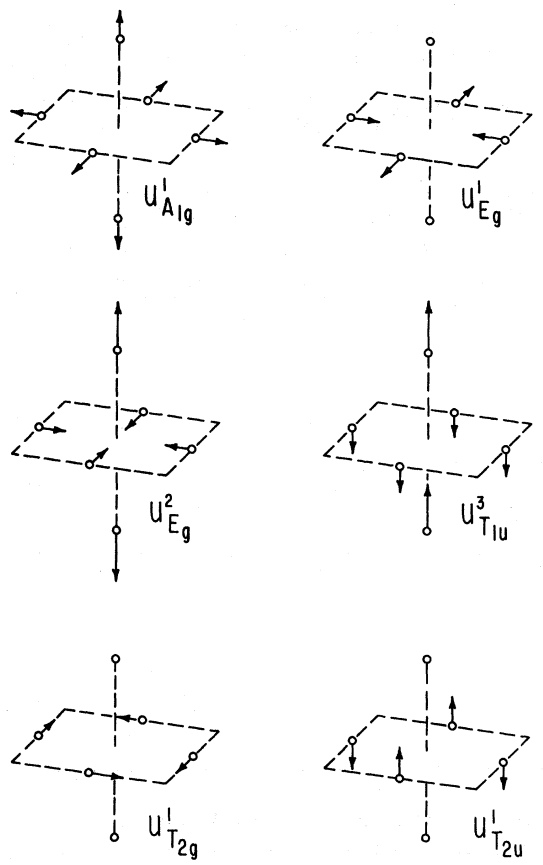

FIG. 2. Pictorial representations of the six symmetry coordinates listed in Eq. (1).

$$(\mathcal{H}_I)_{pp} = -\sum_{\Gamma,\nu} F^p_{\Gamma,\nu} u^\nu_\Gamma . \tag{3}$$

The summation is over representations Γ and rows ν of the octahedral group; the u^ν_Γ are the symmetric combinations of nearest-neighbor displacements given by Eqs. (1); and the $F^p_{\Gamma,\nu}$ are the coupling coefficients (with dimensions of a force) when the impurity is in a particular orientation specified by the index p.

The displacement of the lattice ion located at position $a\vec{l}$ is written in second-quantized form as[17]

$$\vec{u}_{\vec{l}} = \sum_{\vec{k},j} \left(\frac{\hbar}{2NM_\kappa \omega_{\vec{k},j}}\right)^{1/2} \vec{v}(\kappa|\vec{k},j)\, e^{ia\vec{k}\cdot\vec{l}} \times (a_{\vec{k},j} + a^\dagger_{-\vec{k},j}) . \tag{4}$$

In an alkali halide the index κ has value 1 or 2 depending on whether the ion at site $\vec{l}$ is positive or negative; the index j runs over the six phonon modes of wave vector $\vec{k}$. The indices κ and j will be suppressed in the following unless required. The polarization vectors $v^\alpha(\kappa|\vec{k},j)$ form a six-dimensional unitary matrix with row index α, κ and column index j. The symmetry coordinates u^ν_Γ can be second quantized by using Eq. (4):

$$u^\nu_\Gamma = \sum_{\vec{k}} \left(\frac{\hbar}{2NM\omega_{\vec{k}}}\right)^{1/2} P^\nu_\Gamma(\vec{v}_{\vec{k}} e^{ia\vec{k}\cdot\vec{l}})(a_{\vec{k}} + a^\dagger_{-\vec{k}}) . \tag{5}$$

Here P^ν_Γ is a projection operator that projects out of the 18 $v^\alpha_{\vec{k}} e^{ia\vec{k}\cdot\vec{l}}$ ($\alpha = x, y, z$; $l = 1, \ldots, 6$) that part which transforms according to Γ, ν. For example

$$P^1_{A_{1g}}(\vec{v}_{\vec{k}} e^{ia\vec{k}\cdot\vec{l}}) = i(\tfrac{2}{3})^{1/2}(v^x_{\vec{k}} \sin ak_x + v^y_{\vec{k}} \sin ak_y + v^z_{\vec{k}} \sin ak_z) , \tag{6a}$$

$$P^1_{T_{1u}}(\vec{v}_{\vec{k}} e^{ia\vec{k}\cdot\vec{l}}) = 3^{-1/2} v^x_{\vec{k}} (2\cos ak_x - \cos ak_y - \cos ak_z) . \tag{6b}$$

The interaction Hamiltonian can then be written

$$(\mathcal{H}_I)_{pp} = \sum_{\vec{k}} W^p_{\vec{k}} (a_{\vec{k}} + a^\dagger_{-\vec{k}}) , \tag{7a}$$

$$W^p_{\vec{k}} = -\sum_{\Gamma,\nu} \left(\frac{\hbar}{2MN\omega_{\vec{k}}}\right)^{1/2} F^p_{\Gamma,\nu} P^\nu_\Gamma(\vec{v}_{\vec{k}} e^{ia\vec{k}\cdot\vec{l}}) . \tag{7b}$$

We are interested in the zero-temperature renormalization factor for tunneling between two orientations p and p'. As discussed in Sec. I, if the bare tunneling matrix element for this reorientation, obtained from $\mathcal{H}_T$, is Δ_0, then the reorientation dynamics will be governed by a "renormalized" matrix element Δ, given by[7,9]

$$\Delta^2 = \Delta_0^2 \exp\left(-\sum_{\vec{k}} \frac{|W^p_{\vec{k}} - W^{p'}_{\vec{k}}|^2}{(\hbar\omega_{\vec{k}})^2}\right) \tag{8a}$$

$$= \Delta_0^2 e^{-W_0} \tag{8b}$$

The exponent in Eq. (8a) can be written

$$-\sum_{\Gamma,\Gamma',\nu,\nu'} (F^p_{\Gamma,\nu} - F^{p'}_{\Gamma,\nu})(F^p_{\Gamma'\nu'} - F^{p'}_{\Gamma'\nu'}) \left(\sum_{\vec{k}} \frac{1}{2MN\hbar\omega^3_{\vec{k}}} P^\nu_\Gamma(\vec{v}_{\vec{k}} e^{ia\vec{k}\cdot\vec{l}})^* P^{\nu'}_{\Gamma'}(\vec{v}_{\vec{k}} e^{ia\vec{k}\cdot\vec{l}})\right) . \tag{9}$$

The sum in brackets over all $\vec{k}$ in the Brillouin zone vanishes unless $\Gamma = \Gamma'$, $\nu = \nu'$. Thus

$$\Delta^2 = \Delta_0^2 \exp\left(-\sum_{\Gamma,\nu} (F^p_{\Gamma,\nu} - F^{p'}_{\Gamma,\nu})^2 D_\Gamma\right) , \tag{10a}$$

$$D_\Gamma = \sum_{\vec{k}} (2MN\hbar\omega^3_{\vec{k}})^{-1} |P^\nu_\Gamma(\vec{v}_{\vec{k}} e^{ia\vec{k}\cdot\vec{l}})|^2 . \tag{10b}$$

This is the desired result. The F's in Eq. (10a) depend on the particular orientation and properties of the impurity but the D_Γ are characteristic of the host lattice and can be tabulated for a given alkali halide. The D_Γ are independent of the row index ν; thus for each alkali halide one has to calculate at most ten numbers (five different rep-

resentations for either positive or negative nearest neighbors).

III. EVALUATION OF D_Γ

If Eq. (10b) is used directly to evaluate the D_Γ, one can choose any row ν of the representation Γ, but it is then necessary to integrate over the complete Brillouin zone. Much calculating time can be saved if the integrand is first symmetrized by averaging over ν; then it is only necessary to integrate over the segment of the zone: $k_x \geq k_y \geq k_z \geq 0$. With all indices restored, Eq. (10b) becomes

$$D_\Gamma(\kappa) = \sum_{\vec{k},j,\nu} (2SM_\kappa N\hbar\omega^3_{\vec{k},j})^{-1} \left| P^\nu_\Gamma[\vec{v}(\kappa|\vec{k},j)e^{i\alpha\vec{k}\cdot\vec{l}}] \right|^2 . \tag{11}$$

Here, S is the dimensionality of the representation Γ. The explicit formulas used in the numerical evaluation are as follows, using the abbreviated notation $A_{\vec{k}} \equiv (MN\hbar\omega^3_{\vec{k}})^{-1}$, $v^x \equiv v^x(\kappa|\vec{k},j)$, $s^x \equiv \sin ak_x$, $c^x \equiv \cos ak_x$:

$$D_{A_{1g}} = \frac{1}{3}\sum_{\vec{k}} A_{\vec{k}}(v^z s^z + v^x s^x + v^y s^y)^2 , \tag{12a}$$

$$D_{E_g} = \frac{1}{6}\sum_{\vec{k}} A_{\vec{k}}[(v^x s^x - v^y s^y)^2 + (v^y s^y - v^z s^z)^2 + (v^z s^z - v^x s^x)^2] , \tag{12b}$$

$$D_{T_{1u}} = \frac{1}{18}\sum_{\vec{k}} A_{\vec{k}}[(v^z)^2(2c^z - c^y - c^x)^2 + (v^x)^2(2c^x - c^z - c^y)^2 + (v^y)^2(2c^y - c^z - c^x)^2] , \tag{12c}$$

$$D_{T_{2g}} = \frac{1}{6}\sum_{\vec{k}} A_{\vec{k}}[(v^y s^x + v^x s^y)^2 + (v^z s^y + v^y s^z)^2 + (v^x s^z + v^z s^x)^2] , \tag{12d}$$

$$D_{T_{2u}} = \frac{1}{6}\sum_{\vec{k}} A_{\vec{k}}[(v^z)^2(c^x - c^y)^2 + (v^x)^2(c^y - c^z)^2 + (v^y)^2(c^z - c^x)^2] . \tag{12e}$$

The evaluation of these formulas requires knowledge of the phonon spectrum and polarization vectors. We decided to use the standard nonbreathing shell model[18,19] to obtain this information because input parameters obtained from a least-squares fit of the phonon spectrum to neutron-diffraction data are now available for almost all the alkali halides. It is difficult to check whether the simple shell model gives very accurate results for the $\vec{v}_k$; uncertainty about this point must be regarded as a possible source of inaccuracy in the numbers calculated here. The integrations are done by summing over 2000 points in $\frac{1}{48}$ of the Brillouin zone (BZ); trial runs using a much larger number of points change the result by 1% or less. Values of the D_Γ obtained in this way for positive and negative nearest neighbors are listed in Tables I and II, respectively. The source of the input data for the shell-model calculation is also given in Table I.[20-24] In all cases except NaBr the neutron-diffraction data were taken at (80–100)°K. These temperatures are low enough so that properties such as elastic constants do not change significantly down to the 1°K range where most reorientation experiments are done. In the case of NaBr the only data available to us was obtained at room temperature; consequently we regard the results for this material as less reliable than for the others.

TABLE I. Positive nearest neighbors.

Material	$D_{A_{1g}}$	D_{E_g}	$D_{T_{1u}}$ (10^8 dyn^{-2})	$D_{T_{2g}}$	$D_{T_{2u}}$
NaCl[a]	3.69	8.84	6.74	8.57	8.67
NaBr[b]	5.79	13.5	11.8	14.3	14.1
NaI[c]	8.46	19.4	16.7	22.1	20.5
KCl[a]	6.03	12.5	9.87	14.9	14.1
KBr[b]	8.29	16.6	16.2	24.3	22.7
KI[d]	12.5	22.6	28.3	39.6	36.5
RbCl[a]	9.44	19.8	17.7	25.5	24.0
RbBr[e]	11.9	23.5	21.2	32.7	30.4
RbI[f]	17.8	28.2	43.7	52.4	48.1

[a]Reference 20.
[b]Reference 23.
[c]Reference 19.
[d]Reference 24.
[e]Reference 21.
[f]Reference 22.

TABLE II. Negative nearest neighbors.

Material	$D_{A_{1g}}$	D_{E_g}	$D_{T_{1u}}$ (10^8 dyn^{-2})	$D_{T_{2g}}$	$D_{T_{2u}}$
NaCl	3.74	8.23	5.12	7.83	7.45
NaBr	7.96	16.1	11.2	16.0	15.7
NaI	12.6	28.7	18.7	26.9	25.9
KCl	6.23	11.4	11.0	15.3	14.0
KBr	12.2	21.5	21.2	29.7	28.6
KI	19.0	30.4	33.5	46.8	43.6
RbCl	7.76	13.7	15.0	22.5	19.7
RbBr	12.9	23.0	26.3	35.4	32.4
RbI	16.5	32.0	34.6	48.7	46.6

IV. REDUCED COUPLING COEFFICIENTS

The D_Γ calculated in the previous section are useful only if the coupling constants $F^{p}_{\Gamma,\nu}$ can be estimated from either a microscopic calculation or from experiment. We choose as a first step to relate the $F^{p}_{\Gamma,\nu}$ to a minimum set of reduced coupling coefficients which do not depend on the specific orientation p at the impurity. The quantity W_0 introduced in Eq. (8b) can be written

$$W_0 = \sum_\Gamma W_\Gamma , \tag{13a}$$

$$W_\Gamma = D_\Gamma \sum_\nu (F^{p}_{\Gamma,\nu} - F^{p'}_{\Gamma,\nu})^2 . \tag{13b}$$

In order to calculate the W_Γ for all the possible reorientations of [100]-, [110]-, or [111]-directed impurities, we first specify the orientation p by direction cosines with respect to the crystallographic axes: η_x, η_y, η_z. The interaction energy $\mathcal{H}_I$ is an invariant under the operations of O_h. We introduce five independent parameters f_Γ, one parameter for each irreducible representation, and form the invariant:

$$\begin{aligned}(\mathcal{H}_I)_{pp} = &- f_{A_{1g}} u^1_{A_{1g}} - f_{E_g}[(\eta_x^2 - \eta_y^2) u^1_{E_g} + 3^{-1/2}(2\eta_z^2 - \eta_x^2 - \eta_y^2) u^2_{E_g}] \\ &- f_{T_{1u}}(\eta_x u^1_{T_{1u}} + \eta_y u^2_{T_{1u}} + \eta_z u^3_{T_{1u}}) - f_{T_{2g}}(\eta_x\eta_y u^1_{T_{2g}} + \eta_y\eta_z u^2_{T_{2g}} + \eta_z\eta_x u^3_{T_{2g}}) \\ &- f_{T_{2u}}[\eta_z(\eta_x^2 - \eta_y^2) u^1_{T_{2u}} + \eta_x(\eta_y^2 - \eta_z^2) u^2_{T_{2u}} + \eta_y(\eta_z^2 - \eta_x^2) u^3_{T_{2u}}] .\end{aligned} \tag{14}$$

Comparing Eq. (14) with Eq. (3) gives the $F^{p}_{\Gamma,\nu}$ in terms of the f_Γ and the direction cosines. If we choose two orientations p and p' we can use Eq. (13b) to obtain the W_Γ in the form

$$W_\Gamma = C_\Gamma(p, p') f_\Gamma^2 D_\Gamma , \tag{15}$$

where the C_Γ are numerical coefficients of order unity which depend on the direction cosines of p and p'. We note that all $C_{A_{1g}} = 0$, since the interaction for the "breathing" mode is independent or orientation. The $C_{T_{1u}}$ are especially simple to obtain because the three components of the T_{1u} representation transform like a vector; $C_{T_{1u}}$ depends only on the angle θ separating the two orientations:

$$C_{T_{1u}}(\theta) = 4\sin^2\tfrac{1}{2}\theta . \tag{16}$$

The C_Γ coefficients for the four representations are listed in Table III. In those cases where a C_Γ is zero for all reorientations of a particular impurity type, this is indicated by dashes in the appropriate column of Table III.

Reference to Table III shows that couplings of certain symmetry tend to favor reorientation through some angles and inhibit others. For example, for [100] impurities, a large f_{E_g} inhibits 90° tunneling in comparison to 180° tunneling, while the reverse is true for large $f_{T_{1u}}$. The most interesting case is [110] where the relative rate for 60°-vs-90° reorientation is an important experimental question, and where couplings of all four symmetry types enter. Table III shows that large f_{E_g} and $f_{T_{2u}}$ favor a faster rate for 90° tunneling while large $f_{T_{1u}}$ and $f_{T_{2g}}$ favor a faster 60° rate. Thus the relative magnitudes of these coupling parameters are of considerable importance.

TABLE III. Coefficients C_Γ used in Eq. (15).

Impurity type	Reorientation θ (deg)	C_{E_g}	$C_{T_{1u}}$	$C_{T_{2g}}$	$C_{T_{2u}}$
[100]	90	4	2	...	...
	180	0	4	...	...
[110]	60	1	1	$\frac{1}{2}$	$\frac{3}{4}$
	90	0	2	1	$\frac{1}{2}$
	120	1	3	$\frac{1}{2}$	$\frac{1}{4}$
	180	0	4	0	1
[111]	70.5	...	$\frac{4}{3}$	$\frac{8}{9}$	...
	109.5	...	$\frac{8}{3}$	$\frac{8}{9}$	...
	180	...	4	0	...

V. RELATION BETWEEN f_Γ AND MEASURABLE QUANTITIES

In order to make use of the preceding results, one must be able to estimate the f_Γ. The approach taken here is to relate these quantities where possible to experimentally accessible quantities: the electric-dipole moment and various stress-splitting factors. The simplest case is that of the electric dipole. The energy of interaction between a dipole moment $\vec{p}$ pointing along the x axis and the six nearest neighbors of charge e and distance a is

$$\mathcal{H}_I = -(12)^{1/2} pea^{-3} u^1_{T_{1u}} . \tag{17}$$

Comparing with Eqs. (14) and (13b) gives

$$f_{T_{1u}} = (12)^{1/2} pea^{-3} . \tag{18}$$

There exists much uncertainty as to the connection between the value of p appearing in Eq. (18) and the effective dipole moment determined from the interaction energy with an external electric field.

(This latter quantity is usually called the "uncorrected" dipole moment p_u.) Based on the work of Mahan[25] we proposed in Ref. 6 the relation

$$p = (\epsilon_\infty + 2)(\epsilon_0 + 2)^{-1}\epsilon_\infty^{-1} p_u \ ; \tag{19}$$

here ϵ_0 and ϵ_∞ are the low- and high-frequency dielectric constants of the host. This relation is obtained by assuming that a calculation for the interaction between a dipole and a point charge embedded in a polarizable continuum is valid for nearest neighbors; therefore its usefulness is somewhat questionable. This point is a subject of current study.

The connection to the stress-splitting factors is obtained by noting that the modes E_g and T_{2g} correspond to components of the local strain e_{ij}:

$$u^1_{E_g} = a(e_{xx} - e_{yy}) \ ; \tag{20a}$$

$$u^2_{E_g} = 3^{-1/2} a(2e_{zz} - e_{xx} - e_{yy}) \ ; \tag{20b}$$

$$u^{1,2,3}_{T_{2g}} = a e_{xy,yz,zx} \ . \tag{20c}$$

If we now assume that the local elastic constants of the host are not changed by the presence of the impurity, we can relate the local strain to an external stress σ_{ij}. The components we need are

$$u^2_{E_g} = 3^{-1/2} a(C_{11} - C_{12})^{-1}(2\sigma_{zz} - \sigma_{xx} - \sigma_{yy}) \ , \tag{21a}$$

$$u^{1,2,3}_{T_{2g}} = a C_{44}^{-1} \sigma_{xy,yz,zx} \ . \tag{21b}$$

Here C_{11}, C_{12}, C_{44} are the elastic constants of the host. It should be emphasized that Eqs. (21) are approximate insofar as they assume that the macroscopic elastic constants can be used to obtain the displacements of the nearest neighbors.

Consider now an experiment in which a uniaxial stress S_1 is applied along a [100] axis or a stress S_2 is applied along a [111] axis. In the first case the only nonzero σ_{ij} is

$$\sigma_{zz} = S_1 \ ,$$

while in the second all σ_{ij} are equal to

$$\sigma_{ij} = \tfrac{1}{3} S_2 \ .$$

From Eq. (14) the interaction energy with the impurity is

$$\mathcal{H}_I = -\tfrac{2}{3} a f_{E_g}(C_{11} - C_{12})^{-1}(2\eta_z^2 - \eta_x^2 - \eta_y^2) S_1 - \tfrac{1}{3} a f_{T_{2g}} C_{44}^{-1}(\eta_x\eta_y + \eta_y\eta_z + \eta_z\eta_x) S_2 \ . \tag{22}$$

Examination of Eq. (22) shows that for any impurity-system application of an external stress S_1 or S_2 results in splitting of the originally degenerate levels into at most two sets of levels separated by energy E. The stress-splitting factors α_1, α_2 are proportionality factors defined by $E = \alpha_1 S_1$, $E = \alpha_2 S_2$.[26] For [100]-directed impurities, we find $\alpha_2 = 0$ and

$$\alpha_1 = 2a f_{E_g}(C_{11} - C_{12})^{-1} \ . \tag{23}$$

TABLE IV. Coefficients b_Γ used in Eqs. (26a)–(26c).

Impurity type	Reorientation θ (deg)	b_{E_g}	$b_{T_{1u}}$	$b_{T_{2g}}$
[100]	90	1	24	•••
	180	0	48	•••
[110]	60	1	12	$\frac{9}{2}$
	90	0	24	9
	120	1	36	$\frac{9}{2}$
	180	0	48	0
[111]	70.5	•••	16	$\frac{9}{2}$
	109.5	•••	32	$\frac{9}{2}$
	180	•••	48	0

For [110]-directed impurities

$$\alpha_1 = a f_{E_g}(C_{11} - C_{12})^{-1} \ , \tag{24a}$$

$$\alpha_2 = \tfrac{1}{3} a f_{T_{2g}} C_{44}^{-1} \ . \tag{24b}$$

For [111]-directed impurities, $\alpha_1 = 0$ and

$$\alpha_2 = \tfrac{4}{9} a f_{T_{2g}} C_{44}^{-1} \ . \tag{25}$$

Equations (15), (18), and (23)–(25) and Table III can now be combined to give the final result for the W_Γ:

$$W_{E_g} = b_{E_g}(p, p') a^{-2}(C_{11} - C_{12})^2 \alpha_1^2 D_{E_g} \ , \tag{26a}$$

$$W_{T_{1u}} = 48 \sin^2 \tfrac{1}{2}\theta \, e^2 a^{-6} p^2 D_{T_{1u}} = b_{T_{1u}}(p, p') e^2 a^{-6} p^2 D_{T_{1u}} \ , \tag{26b}$$

$$W_{T_{2g}} = b_{T_{2g}}(p, p') a^{-2} C_{44}^2 \alpha_2^2 D_{T_{2g}} \ . \tag{26c}$$

The numerical coefficients $b_\Gamma(p, p')$ are listed in Table IV for all the possible reorientations. Unfortunately, there does not seem to be a way to relate $f_{T_{2u}}$ to an experimentally accessible quantity. It is probably reasonable to assume that coupling of this symmetry is small, so that the contribution of $W_{T_{2u}}$ to W_0 can be neglected.

There is one class of impurity for which $W_{T_{1u}}$ and $W_{T_{2u}}$ are identically zero. Molecular impurities such as[12] O_2^- or[27] N_2^- are symmetric under inversion through the lattice site. Therefore all couplings of odd symmetry are forbidden.

VI. COMPARISON WITH EXPERIMENT

The results obtained above can be used to compare differing relaxation rates (i.e., differing values of Δ) in two different ways: (i) comparison of rates for a given impurity in different host materials; (ii) comparison of rates for several types of reorientation (i.e., 60°-vs-90° reorientation) for an impurity in a single-host material. In this section we will consider both types of experiment.

Kapphan has measured the one-phonon 90° reorientation rate of the [100]-directed impurity OH^- in several alkali-halides using two complementary

TABLE V. Relaxation of [100]-directed OH^-.

Quantity	Unit	KCl	RbCl	KBr	RbBr	RbI
C_{11}	10^{11} dyn/cm	4.6	4.3	4.2	3.86	3.2
C_{12}	10^{11} dyn/cm	0.58	0.65	0.48	0.47	0.36
C_{44}	10^{11} dyn/cm	0.65	0.49	0.52	0.41	0.29
a	Å	3.14	3.27	3.28	3.42	3.63
w (at 1.3 °K)[a]	$\sec^{-1}$	1.7×10^{7}	2.5×10^{4}	5×10^{3}	1.6×10^{2}	2.5×10^{3}
Q	10^{55} °K^{-3} cm^{-6}	0.641	1.35	1.24	2.00	2.81
α_1	10^{-24} cm^3	5.8	5.0	7.8	8.7	12.0
Δ[b]	°K	0.25	7.5×10^{-3}	2.3×10^{-3}	3×10^{-4}	7×10^{-4}
P_u	eÅ	0.95	1.0	0.9	1.0	1.0
$\bar{\epsilon}$		3.44	3.49	3.50	3.55	3.75
$W_{T_{1u}}$		10.0	15.2	11.0	13.4	17.3
W_{E_g}		6.89	6.17	13.0	17.5	25.6
Δ_0[c]	°K	1160	330	374	1540	1.4×10^{6}
w^{theor}(at 1.3 °K)[d]		4.3×10^{5}	6.7×10^{4}	8.0×10^{4}	8.0×10^{3}	1.2×10^{2}

[a]Reference 4. [b]From Eq. (27). [c]From Eq. (30). [d]From Eq. (34).

techniques, "optical" and "caloric."[4] The experimentally observed rates are closely related to the basic transition rate for 90° reorientation of the dipoles, w. The relaxation rates for the "caloric" method, τ_x^{-1}, and the "optical" method, τ_y^{-1}, are related to w by $\tau_x^{-1}=4w$; $\tau_y^{-1}=6w$. As first discussed by Dick,[3] the one-phonon rate w can be written

$$w=\Delta^2\alpha_1^2 TQ\ . \tag{27}$$

Here Δ is the (renormalized) tunneling parameter, α_1 the stress-splitting coefficient, T the temperature, and Q a constant that depends on the properties of the host lattice. Kapphan obtains values of Δ from his experimental relaxation rates by using an expression for Q due to Dick[28]:

$$Q\approx(80\pi\rho\hbar^4)^{-1}(C_{11}-C_{12})^2(2c_l^{-5}+3c_t^{-5})k_B\ . \tag{28}$$

Here ρ is the density, C_{11} and C_{12} are elastic constants, and c_l, c_t are average velocities of long-wavelength longitudinal and transverse phonons. A slight improvement over this expression can be obtained by evaluating the average over the solid angle in $\vec{k}$ space numerically. Thus, instead of Eq. (28), we use

$$Q=(2\pi^2\rho\hbar^4)^{-1}(C_{11}-C_{12})^2k_B^3 \times\sum_j\int d\Omega\,(1/c_j^5)(u_j^x\eta_x-u_j^y\eta_y)^2\ . \tag{29}$$

Here, the integration is over all directions in $\vec{k}$ space; η_x, η_y are direction cosines; the summation j is over the three acoustic modes with velocity c_j and polarization vector $\vec{u}_j$. The $\vec{u}_j$ are normalized three-dimensional vectors obtained by diagonalizing a 3×3 dynamical matrix.[29] Eq. (29) contains a factor of k_B^3 so that both Δ and T in Eq. (27) have units °K.

In the first part of Table V we list the experimental values of w obtained by Kapphan[4] for five host crystals, other required experimental data,[30] values of Q calculated from Eq. (29), and calculated "experimental" values of Δ obtained from Eq. (27). The values of Δ we obtain are quite close to the values obtained by Kapphan using the approximation Eq. (28) for Q. Table V shows that the large range of values for w are indeed due primarily to the range of values for Δ as one goes from one material to another.

We now attempt to fit the "experimental" values of Δ by an expression of the form

$$\Delta=\Delta_0\exp[-\tfrac{1}{2}(W_{T_{1u}}+W_{E_g})]\ , \tag{30}$$

with the expectation that the bare matrix element Δ_0 varies less rapidly with material than does Δ. Using Eqs. (26a), (26b), and Table IV, we find for [100]-oriented impurity and 90° reorientation

$$W_{T_{1u}}=24e^2a^{-6}p^2D_{T_{1u}}\ , \tag{31}$$

$$W_{E_g}=(C_{11}-C_{12})^2\alpha_1^2a^{-2}D_{E_g}\ . \tag{32}$$

The dipole moment p is related to the uncorrected (experimental) value by $p=p_u/\bar{\epsilon}$. Following Eq. (19) we use

$$\bar{\epsilon}=\epsilon_\infty(\epsilon_0+2)/(\epsilon_\infty+2)\ . \tag{33}$$

The data used in the evaluation of $W_{T_{1u}}$ and W_{E_g} and the calculated values are given in Table V.[31–33] We then list calculated values of Δ_0 obtained from Eq. (30). With the exception of RbI, the values of Δ_0 so obtained are within a fairly small range. However these values are unphysically large.

We believe that the unphysical values of Δ_0 indicate that one cannot calculate the factors $W_{T_{1u}}$ and W_{E_g} by using the macroscopic coupling constants α_1 and p_u directly, since the values of the local elastic constants and local dielectric constant

in the vicinity of the impurity may differ from their bulk values. To proceed, we suppose that the local values of α_1 and p_u are reduced from their macroscopic values by factors C_α and C_p, respectively, and that these factors are independent of material. The theoretical expression for the reorientation rate then becomes

$$w = C_\alpha^2 \alpha_1^2 QT\Delta_0^2 \exp[-(C_\alpha^2 W_{E_g} + C_p^2 W_{T_{1u}})] . \quad (34)$$

We then choose a reasonable value of Δ_0, 3 °K, and determine C_α and C_p in order to produce the best least-squares fit between experimental and theoretical values of w for the five materials studied. The best fit is obtained with $C_\alpha = 0.63$, $C_p = 0.71$. These correction factors are close to unity, and it is very reasonable that the microscopic coupling constants could differ from the observed values by this order of magnitude.

In the final row of Table V, we list the calculated rates for the five materials. The agreement with the experimental rates is not particularly good, but the wide range of rates is reproduced qualitatively. In view of the assumptions that Δ_0, C_α, and α_p are independent of material we regard the agreement as satisfactory.

A second set of experiments that we discuss involves the reorientation of Ag^+ ions in RbCl and RbBr. As discussed in Ref. 15 and in the accompanying paper by Jiminez and Lüty, [16] Ag^+ sits off center along a [110] direction in these materials. Consequently reorientation can occur between [110] directions separated by either 60° or by 90°. Kapphan and Lüty[15] could determine the reorientation rate for the two processes individually as a function of temperature. They find that for both materials the rate for 90° reorientation is much larger than the 60° rate. If the reorientation is due to tunneling, this implies that the tunneling matrix element for 90° reorientation is larger than the 60° matrix element, contrary to any reasonable expectation for a "bare" tunneling matrix element (i.e., any reasonable static potential of octahedral symmetry would not yield such a result. [12]) As Kapphan and Lüty propose, a possible explanation is that coupling of the impurity to a tetragonal distortion of the lattice (i.e., a mode of E_g symmetry) could result in strong renormalization of the 60° matrix element but would have no effect on 90° tunneling. Since the stress coupling coefficients[16] α_1, α_2 and the electric-dipole moments[15] for the two systems have been measured, we can estimate the renormalization factors for the 60° and 90° processes and check whether the proposed mechanism is reasonable.

One difficulty of applying the analysis of this paper to the reorientation of a heavy ion such as Ag^+ is that the "bare" matrix element Δ_0 is itself very small. Consequently, reorientation may take place via thermal activation, rather than by tunneling, even at low temperatures. The temperature dependence of the reorientation rate is the most reliable method for distinguishing the two mechanisms. For the system RbCL: Ag^+, Kapphan and Lüty find a T^5 dependence for the 60° reorientation rate for $T > 1.8$ °K. This dependence is consistent with multiphonon-assisted tunneling.[7] Bridges has obtained the temperature dependence of the 90° reorientation in this system down to $T = 1.4$ °K using a paraelectric-resonance-saturation technique and obtains results consistent with one-phonon relaxation. [34] We conclude therefore that both the slow 60° and the fast 90° reorientations of RbCl: Ag^+ are due to phonon-assisted tunneling in the temperature range of interest ($T < 4$ °K).

In RbBr: Ag^+ the temperature dependence of the 90° relaxation rate can be fit by a multiphonon tunneling model for temperatures below 5 °K. At about this temperature, the data of Kapphan and Lüty indicate that a thermally activated process takes over, giving an exponential rate for higher temperatures. The same data indicate that the 60° rate is fit very well by an exponential temperature dependence. Thus, the only conclusion that can be drawn about the 60° tunneling rate is that it is too slow to be measured.

In analyzing these experiments we again suppose that the variation in relaxation rates is due primarily to the renormalization of the tunneling matrix elements. Using Eqs. (13a), (26), and Table IV we find for 90° reorientation of a [110]-oriented impurity,

$$W_0^{90} = 9\alpha_2^2 (C_{44}^2/a^2) D_{T_{2g}} + 24(e^2p^2/a^6) D_{T_{1u}} . \quad (35)$$

Similarly, the 60° rate is

$$W_0^{60} = \alpha_1^2 [(C_{11} - C_{12})^2/a^2] D_{E_g} + \tfrac{9}{2}\alpha_2^2 (C_{44}^2/a^2) D_{T_{2g}} + 12(e^2p^2/a^6) D_{T_{1u}} . \quad (36)$$

If the first term in Eq. (36) is large, this would result in a reduction in magnitude of the 60° matrix element compared to the 90° element.

In Table VI we present the experimental information needed to check whether the four relaxation rates (60° and 90° reorientation in RbCl and RbBr) can be related to the appropriate renormalization factors e^{-W_0}. The transition rates w^{90} and w^{60} are estimated one-phonon rates obtained by extrapolating the experimental results for τ_{opt}^{90} and τ_{opt}^{60} to 1 °K and using the relations

$$w^{90} = (4\tau_{opt}^{90})^{-1} , \quad (37a)$$

$$w^{60} = (6\tau_{opt}^{60})^{-1} . \quad (37b)$$

The dipole moments p_u are "uncorrected" values. We found it most useful to evaluate the T_{1u} contri-

bution to the W_0 using p_u in place of p, and then multiplying the answer by $(p/p_u)^2$. The remaining quantities needed to evaluate Eqs. (35) and (36) are obtained from Tables V and II. The numerical results for the two terms in Eq. (35) and the three terms in Eq. (36) are listed in Table VI.

The renormalization factors e^{-W_0} are plotted in Fig. 3 as a function of p/p_u. The results predict that the 60° tunneling motion in RbBr : Ag^+ is essentially frozen out by the lattice E_g distortion, in agreement with experiment. Further, for values of p/p_u between 0.3 and 0.4 the relative order of the four calculated renormalization factors is in agreement with the observed relaxation rates. The value of p/p_u obtained from Eq. (33) is about 0.29 for both RbCl and RbBr, while the simple Lorentz local-field correction $3/(\epsilon_0+2)$ gives a value of about 0.43 in both materials. Thus the choice of p/p_u that seems to give the best agreement with experiment is reasonable. For $p/p_u \sim 0.35$ the relative spacing of the renormalization factors is in fair agreement with the four experimental relaxation rates listed in Table VI.

A final application of the present theory is a comparison of relaxation rates and renormalization factors for the paraelastic defects O_2^- and N_2^- in the materials KCl and KI. These are [110]-oriented impurities which can reorient via 60° or 90° tunneling, just as in the case of Ag^+. However, these homonuclear defects have no electric-dipole moment, so there can be no contribution to W_0 of T_{1u} symmetry. The stress-splitting factors and one-phonon relaxation rates for O_2^- have been measured by Känzig[35] and Pfister and Känzig.[36] Silsbee and Bojko[27] have measured splitting factors and *thermally activated* reorientation rates for N_2^-; they argue pursuasively, however, that the *relative* rate of 60° to 90° relaxation is indicative of the relative tunneling matrix elements for the two processes.

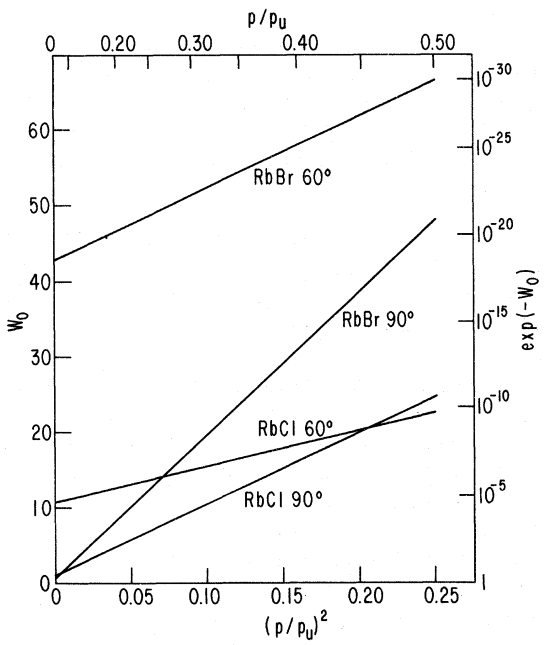

FIG. 3. Renormalization factor W_0 as a function of the ratio p/p_u for RbCl : Ag^+ and RbBr : Ag^+.

The renormalization factors W_0^{90} and W_0^{60} can again be calculated using Eqs. (35) and (36); the results are given in Table VII. For three out of the four experiments studied, the relative rate of 60° to 90° reorientation correlates well with the difference between W_0^{90} and W_0^{60}. There is a glaring discrepancy, however, in the case of O_2^- in KCl. In this case the 60° relaxation rate is much *faster* than the 90° rate, while the calculated value of $W_0^{60} - W_0^{90}$ predicts just the opposite. We are

TABLE VI. Relaxation of [110]-directed Ag^+.

Quantity	Unit	RbCl	RbBr
w^{90} (at 1.0 °K)	sec^{-1}	2.5×10^4	1×10^{-2}
w^{60} (at 1.0 °K)	sec^{-1}	10	$<10^{-6}$
p_u	eÅ	0.78	0.95
α_1	10^{-24} cm^3	7.8	13.7
α_2	10^{-24} cm^3	1.82	3.5
$W^{90}_{T_{2g}}$		0.86	0.57
$W^{90}_{T_{1u}}$		$47.4(p/p_u)^2$	$94.5(p/p_u)^2$
$W^{60}_{E_g}$		10.1	42.3
$W^{60}_{T_{2g}}$		0.43	0.29
$W^{60}_{T_{1u}}$		$94.5(p/p_u)^2$	$189(p/p_u)^2$

TABLE VII. Relaxation of O_2^- and N_2^-.

Quantity	Unit	KCl	KI
O_2^-			
w^{90} (at 1.0 °K)[a]	10^{-3} sec^{-1}	1.9	2.5
w^{60} (at 1.0 °K)[a]	10^{-3} sec^{-1}	25	2.3
α_1[b]	10^{-24} cm^3	8.15	6.18
α_2[b]	10^{-24} cm^3	5.00	12.50
W_0^{90}		1.4	6.1
W_0^{60}		14	3.9
N_2^-			
w^{90} (at 20 °K)[c]	10^6 sec^{-1}	20.4	$\gg w^{60}$
w^{60} (at 20 °K)[c]	10^6 sec^{-1}	0.91	7.45
α_1[d]	10^{-24} cm^3	5.59	9.48
α_2[d]	10^{-24} cm^3	8.55	14.5
W_0^{90}		4.2	8.2
W_0^{60}		8.5	17.8

[a]From Table I of Ref. 36. [c]From Table II of Ref. 27.
[b]From Table II of Ref. 35. [d]From Table I of Ref. 27.

unable to account for the large discrepancy in this case. A possible explanation is that since the lattice spacing in KCl is very small, the tunneling matrix elements $\Delta_0(60°)$ and $\Delta_0(90°)$ might differ greatly in magnitude.

VII. DISCUSSION

The results of Sec. VI indicate that general trends in relaxation rates can be understood using the calculations described in this paper, but that quantitative agreement is not possible at this point. We believe there are three major reasons for the difficulty:

(a) The most trivial problem is that there is no *a priori* reason to suppose that the "bare" tunneling matrix element Δ_0 is relatively constant for different materials or for different reorientations in the same material. We suggest that this problem occurs in $KCl:O_2^-$. Variation of this parameter by a factor of 10 would lead to a 2 order-of-magnitude variation in relaxation rates, thus eliminating any hope of quantitative correlation between these rates and the renormalization factors.

(b) All of our comparisons with experiment have involved an attempt to determine the microscopic coupling constants f_Γ from the observables α_1, α_2, p_u. Relations such as Eqs. (23)–(25) involve macroscopic elastic constants C_{11}, C_{12} and C_{44}. In reality, the elastic constants relating the relative motion of the impurity and its nearest neighbors in the presence of an external uniaxial stress can differ from the macroscopic values, thus making it impossible to obtain the f_Γ with any certainty. Further, we have been forced to assume $f_{T_{2u}} = 0$, since this coupling coefficient cannot be determined from any macroscopic measurement.

Similar difficulties arise in attempting to obtain $f_{T_{1u}}$ from p_u. We have assumed that the entire force of this symmetry is due to the electric-dipole moment of the impurity. This neglects the possibility of short-range pseudodipolar forces which do not couple to an external electric field, but can contribute to $f_{T_{1u}}$. Further, the attempt to include the effects of lattice polarization in calculating the electric field due to the impurity dipole via Eq. (19) is probably inaccurate for nearest neighbors. The difficulties discussed here led us to include the correction factors C_α and C_p in Eq. (34) to account for the uncertainties in α_1 and p.

(c) The calculation of the D_Γ in Tables I and II depends on several assumptions whose validity can be questioned. The most important of these is that the phonon spectrum and the decomposition of the motion of the nearest neighbors into normal modes of the perfect lattice is not affected by the presence of the defect. Changes in local spring constants due to the impurity can lead to local or resonance modes which modify Eq. (5) and the resulting expression for the D_Γ, Eq. (10b). Such effects of nonlinear coupling between the impurity and the lattice depend on the details of the system and are difficult to estimate without a detailed microscopic model.

Within the linear approximation used, we believe the values of the D_Γ in Tables I and II are accurate to within about 15%. We checked the results against two possible sources of error. In the shell-model calculations, the impurity was assumed to couple to the displacements of the *cores* of the nearest neighbors. It is probably more reasonable to let the impurity couple to the *shell* coordinates. We recalculated the D_Γ with shell coupling and found agreement to about 5% with the original calculations. For the case of electric-dipole coupling $D_{T_{1u}}$, one should allow coupling beyond nearest neighbors, falling off as r^{-3}. This was done for our calculation of W_0 in $RbBr:OH^-$.[6] This affects $D_{T_{1u}}$ by about 10%, so it is not significant compared to the other uncertainties.

ACKNOWLEDGMENT

The authors are indebted to Dr. F. Bridges for several helpful discussions and for communicating results on low-temperature relaxation rates in $RbCl:Ag^+$.

*Work supported in part by NSF Grant No. GH-34439.

[1]R. Pirc, B. Zeks, and P. Gosar, J. Phys. Chem. Solids 27, 1219 (1966).

[2]L. A. Vredevoe, Phys. Rev. 153, 312 (1967).

[3]B. G. Dick, Phys. Status Solidi 29, 587 (1968).

[4]S. Kapphan, J. Phys. Chem. Solids 35, 621 (1974).

[5]B. G. Dick and D. Strauch, Phys. Rev. B 2, 2200 (1970).

[6]H. B. Shore and L. M. Sander, Phys. Rev. B 6, 1551 (1972).

[7]L. M. Sander and H. B. Shore, Phys. Rev. B 3, 1472 (1971).

[8]H. B. Shore and L. M. Sander, Solid State Commun. 9, 95 (1971).

[9]P. Gosar and R. Pirc, in *Proceedings of the Fourteenth Colloque Ampère, Ljublijana*, 1966, edited by R. Blinc (North-Holland, Amsterdam, 1967), p. 636.

[10]R. Pirc and P. Gosar, Phys. Kondens. Mater. 9, 377 (1969).

[11]H. B. Shore, Phys. Rev. Lett. 17, 1142 (1966).

[12]R. H. Silsbee, J. Phys. Chem. Solids 28, 2525 (1967).

[13]A. S. Nowick and W. R. Heller, Adv. Phys. 12, 251 (1963).

[14]A. S. Nowick, Adv. Phys. 16, 1 (1967).

[15]S. Kapphan and F. Lüty, Phys. Rev. B 6, 1537 (1972).

[16]R. Jimenez and F. Lüty, preceding paper, Phys. Rev. B 12, 1531 (1975).

[17]See for example, A. A. Maradudin, E. W. Montroll, and G. H. Weiss, in *Solid State Physics*, edited by F. Seitz and D. Turnbull (Academic, New York, 1963), Suppl. 3, Chap. II.

[18]A. D. B. Woods, W. Cochran, and B. N. Brockhouse, Phys. Rev. 119, 980 (1960).
[19]R. A. Cowley, W. Cochran, B. N. Brockhouse, and A. D. B. Woods, Phys. Rev. 131, 1030 (1963).
[20]G. Raunio and S. Rolandson, Phys. Rev. B 2, 2098 (1970); 6, 2511 (1972).
[21]S. Rolandson and G. Raunio, J. Phys. C 4, 958 (1971).
[22]G. Raunio and S. Rolandson, Phys. Status Solidi 40, 749 (1970).
[23]J. S. Reid, T. Smith, and W. J. L. Buyers, Phys. Rev. B 1, 1833 (1970).
[24]G. Dolling, R. A. Cowley, C. Schittenhelm, and I. M. Thorson, Phys. Rev. 147, 577 (1966).
[25]G. D. Mahan, Phys. Rev. 153, 983 (1967).
[26]F. Lüty, J. Phys. (Paris) Suppl. 34, 49 (1973).
[27]R. H. Silsbee and I. Bojko, J. Phys. Chem. Solids 34, 1971 (1973).
[28]B. G. Dick and D. Strauch, Phys. Rev. B 2, 2200 (1970).
[29]See, for example, C. Kittel, *Introduction to Solid State Physics*, 4th ed. (Wiley, New York, 1971), p. 144.
[30]J. T. Lewis, A. Lehoczky, and C. V. Briscoe, Phys. Rev. 161, 877 (1967).
[31]S. Kapphan and F. Lüty, J. Phys. Chem. Solids 34, 969 (1973).
[32]R. Jimenez and F. Lüty, Phys. Status Solidi 52, K47 (1972).
[33]H. Hartel and F. Lüty, Phys. Status Solidi 12, 347 (1965).
[34]F. Bridges (private communication).
[35]W. Känzig, J. Phys. Chem. Solids 23, 479 (1962).
[36]G. Pfister and W. Känzig, Phys. Kondens. Mater. 10, 231 (1969).